Optical beam steering network with multiband capability

Sara Vega, Daniel Nuño, and María C. Santos.

Dept. of Signal Theory and Communications. Universitat Politècnica de Catalunya.
Jordi Girona 1, 08034 Barcelona, Spain.

***Abstract*—A multiwavelength (MW) optical true time delay Network (OTTDN) to feed a phased array antenna (PAA) is presented. Beam steering capabilities can be demonstrated when applying MW tuning. A Dual Electrode Mach Zehnder Modulator (DE-MZM) as radio frequency (RF) external modulating stage allows to tune the operative band avoiding severe Chromatic Dispersion (CD) fading to obtain a flattened response. A working example simulation of a 4 elements array at 8 GHz shows the RF multiband spectral flat response potential of the technique, as well as the network conditions needed for beam steering with free-lobe operation.**

I. Introduction

With the explosive growth of wireless data traffic and the relevance acquired by radar imagers for a variety of applications, e.g. unmanned vehicles, traffic control, security scanning and environmental changes monitoring, the design of phased array antennas (PAA) for beam steering has become a very active research topic. In order to avoid Beam-squint effects, which limit the operative bandwidth of PAA, True Time Delay Networks (TTDN) are employed to feed PAAs [1]. Using photonics in the TTDN is advantageous because it is broadband, low-loss, small footprint and immune to interferences and it allows direct interfacing with high-capacity fiber networks through Radio-over-Fiber (RoF) fronthauling in communication networks [2], [3].

One interesting proposal for Optical TTDN (OTTDN) features a radio frequency (RF) modulated multiwavelength (MW) input propagating over a dispersive line at whose output each PAA element (PAAE) retrieves a single wavelength, which will have acquired a delay that will depend on the dispersion and the wavelength value [4]. The design can be very compact and low-cost by leveraging Wavelength Division Multiplexing-Passive Optical Network (WDM-PONs) components such as thermally-tuned Distributed Feedback Bragg (DFB) lasers and Arrayed Waveguide Gratings (AWG) [5].

A remaining challenge, given the typical narrow band spacing of AWGs optimized for dense WDM (dWDM) optical networks, is related to the large amount of Chromatic Dispersion (CD) required for significant steering of the beam, which may lead to severe CD-induced RF amplitude fading [6]. This effect appears due to the destructive interference caused by the phase shift acquired through CD between photodetected signals at each side of the carrier for Double Side Band (DSB) signals, and it is frequency dependent, limiting the operative RF bandwidth [1].

In this work we propose and analyze the use of a Dual Electrode Mach Zehnder Modulator (DE-MZM) as the modulating stage in a MW OTTDN to shift the CD-fading free band through control of the voltage bias applied to one of the MZ branches, while driving the other branch by the RF signal to radiate. Contrary to alternatives that use optical Single Sideband (SSB) modulation [4], the proposed scheme does not require any specific electrical phase shift between RF signals applied to each of the arms of the DE-MZM, and thus, it is intrinsically wideband. The paper is organized as follows. In Section II the MW tuning is theoretically developed to prove the beam steering principle, while in Section III a DE-MZM modulation is proposed as an alternative to conventional Push-Pull Mach Zehnder Modulator (PP-MZM) to achieve a multiband operation without RF amplitude fading effects. In section IV, an example MW beam steering network is defined, characterized and simulated, demonstrating the predicted capabilities. Finally, section V presents the conclusions.

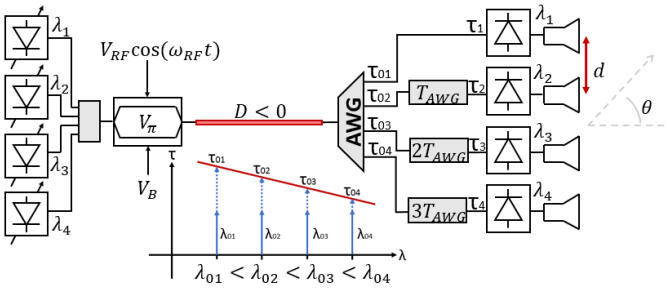

Fig. 1. Setup of OTTDN with DE-MZM.

II. MW Beam Steering Network

Figure 1 shows a sketch of the targeted OTTDN, which resembles the distribution of wavelength channels to users in access WDM-PONs. An array of tunable input lasers, provides a MW signal comprising wavelengths λ_i, $i = 1, 2, ..., N$, numbered in descending order in Figure 1, with N the number of PAA elements. For clarity, and to improve the readability of the manuscript, we will consider in this analysis an even number of array elements, but extension to an odd number is straightforward. After RF modulation with an external DE-MZM, the signal propagates through a dispersive medium for which Dispersion Compensating Fiber (DCF) with negative dispersion coefficient D is conveniently chosen to provide large values of CD in a low volume and over a wide optical band. For the PAA steering, each laser wavelength will be conveniently tuned inside a specific channel of an AWG whose outputs are connected to the PAAEs through an array of N photodetectors. In order to exploit WDM-PON equipment, the C-band of optical communications around $\lambda_0 = 1.55\ \mu m$ is considered.

A. Effect of compensating delays

Owing to CD, the signal fed to every PAAE will have suffered a delay that will depend on the wavelength value inside its channel. Let the center wavelength of each OTTDN channel be $\lambda_{0i} = \lambda_{01} + (i-1)\Delta\lambda_{AWG}$, with $\Delta\lambda_{AWG}$ the AWG channel spacing in wavelength units and λ_{01} the wavelength of the first element of the array (placed at the top in Figure 1), which is considered here the one with the lowest wavelength value, as in Figure 2.

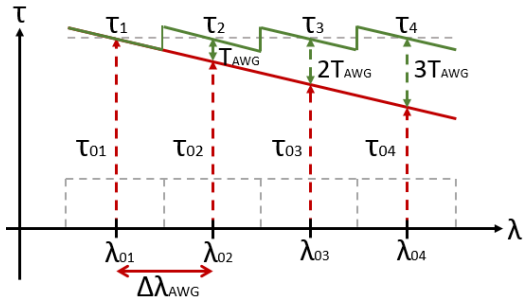

Fig. 2. Group delay distribution against wavelength at the PAAEs before (red) and after (green) compensating delays and relative PAAE channel spacing.

To properly exhaust the channel bandwidth provided by the AWG for a PAA symmetrically steered along both positive and negative angles, when all the input lasers are located at the center of their respective AWG channels the PAA should radiate into the broadside direction. This is accomplished through the compensating delays T_i placed at each PAAE, either before or after the photodetection stage, yielding the overall OTTDN group delay wavelength dependence shown in green in Figure 2.

For lasers in their AWG channel center, the value of the proportional delay in between PAAEs will be $T_{AWG} = |D|L\Delta\lambda_{AWG}$ with D the CD parameter and L the fiber length, so that the compensating delays for each PAAE need to be

$$T_i = (i-1)T_{AWG} \tag{1}$$

In Figure 2, we provide a graphical explanation to illustrate the effect of the compensating delays over the delay dependence on wavelength for this OTTDN structure proposal. The red line delay values represent the delays suffered from the multiwavelength signal modulation with the RF envelope until it is filtered in the PAAEs, τ_{0i}, while the green line represents the delays after the compensating delay stage $\tau_i = \tau_{0i} + T_i$ (check Figure 1).

As seen in Figure 2, τ_{01} may be taken as the absolute timing reference for RF signal arrival at the PAAEs input. The condition for the T_i is then $\tau_i = \tau_{0i} + T_i = \tau_{01}$. The specific T_i values required for a PAA of $N = 4$ elements are summarized in Table I.

B. Geometrical Delays

The far field radiated by the PAA will result from the interference of the individual far field patterns of each PAAE. The far field contribution of each PAAE may be written as

$$E_i = A_i(\theta)\ exp\left(-j2\pi f_{RF}\Delta\tau_{Gi}\right) \tag{2}$$

TABLE I
SUMMARY OF DELAYS AND WAVELENGTHS FOR AN ARRAY OF $N = 4$ PAAE.

i	Compensating Delay (T_i)	Geometrical Delay ($\Delta\tau_{Gi}$)	Wavelength shift ($\delta\lambda_i$)
1	0	$-\frac{3}{2}\frac{d}{c}\sin(\theta)$	$\frac{3}{2}\frac{d}{DLc}\sin(\theta)$
2	T_{AWG}	$-\frac{1}{2}\frac{d}{c}\sin(\theta)$	$\frac{1}{2}\frac{d}{DLc}\sin(\theta)$
3	$2T_{AWG}$	$\frac{1}{2}\frac{d}{c}\sin(\theta)$	$-\frac{1}{2}\frac{d}{DLc}\sin(\theta)$
4	$3T_{AWG}$	$\frac{3}{2}\frac{d}{c}\sin(\theta)$	$-\frac{3}{2}\frac{d}{DLc}\sin(\theta)$

where $A_i(\theta)$ represents the RF signal envelope emitted by each PAAE, f_{RF} is the frequency of the RF signal, and the geometrical delay, for a even number of channels N, may be written in compact form as

$$\Delta\tau_{Gi} = \left(i - \frac{N+1}{2}\right)\frac{d}{c}\sin(\theta) \tag{3}$$

with c the free-space wave velocity, d the a PAA inter-element spacing, and θ the field point angle referred to the PAA broadside direction (see Figure 1). Isotropic radiators will be considered in the analysis, to focus on the PAA response, and therefore $A_i(\theta) = A_i$.

The summation over all the array elements provides the Array Factor $AF = \sum_{i=1}^{N} E_i$, which when convolved with the individual beam pattern of the antennas in the array provides the PAA beam pattern. Lobe-free operation among the full 180^o beam steering of the PAA requires $d < \frac{\lambda_{RF}}{2}$ [7].

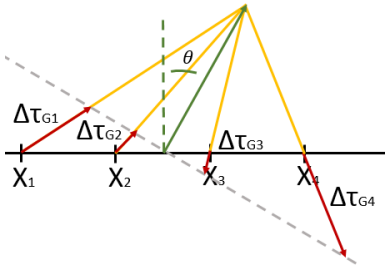

Fig. 3. Geometrical delays for each PAA element and beam direction θ.

The mechanism by which the OTTDN achieves the beam steering towards angle θ consists in providing each PAAE with a RF signal replica which has the same amplitude and a progressive delay that accounts for the geometrical delay due to the PAAE position in the array, see Figure 3. We may then write the complex signal of each PAAE as $A_i = Aexp(-j2\pi f_{RF}\Delta\tau_{Ni})$, with A the common RF amplitude and $\Delta\tau_{Ni}$ its corresponding network delay. The condition for beam steering is that network delays compensate the geometrical delay due to the position in space of each PAAE

$$\Delta\tau_{Gi} + \Delta\tau_{Ni} = 0 \tag{4}$$

Note that while for the network delays we measure the time starting from the first element in the array, here it is preferable to take the center of the array as the time reference due to the geometrical symmetry. As an example, the geometrical delays for a PAA with $N = 4$ elements are summarized in Table I. As long as all the channels are synchronized to the same absolute time reference for the broadside condition,

the relative delays between the PAAEs will define the beam direction by fulfilment of the condition (4).

C. Dispersive Delays

In this section we explain how the OTTDN channel wavelengths need to be tuned in order to achieve the desired beam direction in the PAA. Referring to Figure 3, for radiation into angle θ, the required relative network delays for each PAAE need to be $\Delta\tau_{Ni} = -\Delta\tau_{Gi}$, with $\Delta\tau_{Gi}$ the geometrical delay given by (3). Looking at the group delay curves in Figure 2, the delays acquired by the channels with respect to the absolute delay τ_{01}, are positive when the wavelength is tuned towards the lower wavelength side of the channel and negative otherwise.

The strategy for steering the direction of the PAA beam is to exploit dispersion to achieve the required delays into each PAAE. Therefore, the condition to find the position of the wavelengths into each OTTDN channel for the targeted beam steering angle is

$$\Delta\tau_{Ni} = DL\delta\lambda_i \tag{5}$$

From (3), (4) and (5) we obtain the required phase shift with respect to the channel center for a beam steering angle theta as

$$\delta\lambda_i = \left(i - \frac{N+1}{2}\right)\frac{d}{DLc}\sin(\theta) \tag{6}$$

A useful definition is the relative progressive wavelength shift in between contiguous PAAE for a specific angle of steering $\delta\lambda_0 = \frac{d}{|D|Lc}\sin(\theta)$. See Fig. 4 for a graphical explanation. The PAAEs corresponding wavelengths are expressed in terms of $\delta\lambda_i$ as $\lambda_i = \lambda_{0i} + \delta\lambda_i$.

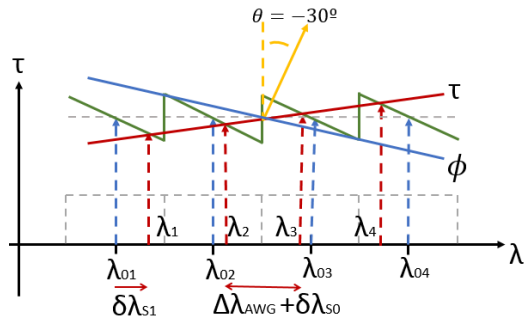

Fig. 4. Relative delays and beam direction for MW tuning.

D. Maximum beam steered angle

The limit for the maximum steered angle will come from the required wavelength shift on any of the OTTDN reaching the limit of the AWG channel half-bandwidth. As seen in preceding sections, the channels that experience the greater wavelength shift are the ones further apart from the PAA center. Therefore, letting $i = N$ in (6) the maximum steered angle with respect to broadside is

$$\theta_{max} = \arcsin\left(\frac{c|D|\Delta\lambda_{AWG}}{d(N-1)}\right) \tag{7}$$

It could be checked that, the higher the number of elements in the PAA or the narrower the AWG channel bandwidth, the larger the CD value needed to fulfill the requirement of a specific maximum steering angle. On the other hand, the higher the CD, the shorter the DFB tuning ranges to achieve the same angle shift, which means better precision and stability required for the tuning. A significant downside of a high value of CD is the RF amplitude fading effect which reduces the RF operative bandwidth [6]. In the next section we describe a method to overcome this effect using the bias voltage of a DE-MZM to shift the position of the dispersion RF notch far from the operating RF band.

III. CD-FADING CONTROL

In a typical configuration, the external RF modulation stage is implemented using a conventional PP-MZM characterized by a 180º phase difference between RF signals applied to each interferometer arm. The usual outcome is a RF DSB amplitude modulation, for which frequency dependent CD-induced RF amplitude fading may cause significant amplitude distortion [6] [8]. A DE-MZM as the RF modulating element of a dispersive OTTDN for PAA beam steering has been proposed in [4] to achieve a SSB modulation of the data by driving each MZ arm with the same RF signal delayed by 90º. However the requirement of a specific electrical phase shift makes the technique intrinsically narrow band [9]. Figure 5 illustrates the choices for the electrical connections in the RF modulation stage of the OTTDN.

In this section we show how the RF amplitude fading typical of dispersive propagation of DSB signals may be avoided at a specific operative frequency through appropriate biasing of a DE-MZM with no specific requirement for RF signal electrical shift, allowing the OTTDN to be tuned over a wide frequency band.

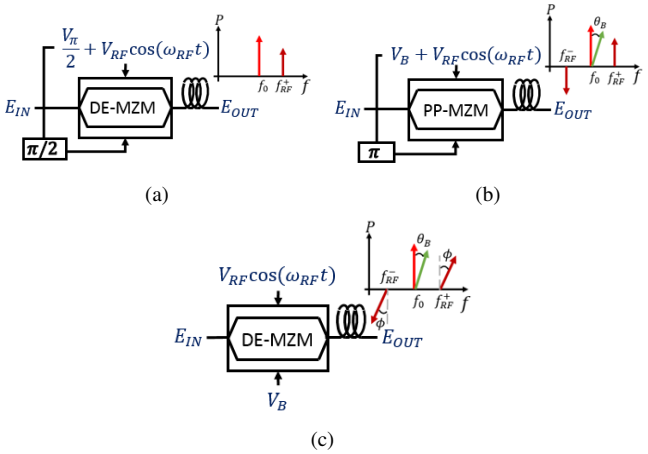

Fig. 5. Sketch of the typical options for external RF modulation at optical frequencies (a) DE-MZM configured for SSB modulation (b) Conventional push-pull MZM, and (c) DE-MZM for CD RF-amplitude free band control using the bias voltage.

Taking as delay reference the time of arrival when all wavelengths are centered into their AWG, τ_{01}, the normalized amplitude field of the signal at each AWG port is given by

$$E_i \approx \cos\left(\frac{\theta_B}{2}\right) + jme^{j\left(\phi - \frac{\theta_B}{2}\right)}\cos\left(2\pi f_{RF}\left(t - \delta\lambda_i DL\right)\right) \tag{8}$$

where $\theta_B = \frac{\pi V_B}{V_\pi}$, and $m = \frac{\pi V_{RF}}{V_\pi}$ with V_B, V_{RF} respectively the biasing voltage and RF signal peak amplitude applied to different the electrodes of the DE-MZM, (see Figure 5(c)), with V_π its half-wave voltage, and $\phi = \frac{\pi DL\lambda_0^2 f_{RF}^2}{c}$

the phase due to CD, with λ_0 the reference wavelength which is conveniently set to the center of the C-band [6]. Note that in (8) the usual small-signal approximation has been applied, i.e. $V_{RF} \ll V_\pi$. From there, the normalized photodetected current at frequency f_R at each PAAE will be

$$I_{PDi} \approx \cos\left(\frac{\theta_B}{2}\right) \sin\left(\frac{\theta_B}{2} - \phi\right) \cos\left(2\pi f_{RF}\left(t - \delta\lambda_i D_L\right)\right) \tag{9}$$

The biasing voltage V_B may be adjusted to compensate the CD-induced amplitude fading given by ϕ, using the condition

$$\theta_B = (2n-1)\pi + 2\phi \tag{10}$$

IV. Simulations

A photonic simulation software (VPI TransmissionMaker) has been used to assess the potential of the technique. A typical AWG spacing of 200 GHz, $\Delta\lambda_{AWG} = 1.6\ nm$, $N = 4$ and $f_{RF} = 8\ GHz$ is considered. Assuming a PAAE spacing of $d = \frac{\lambda}{4}$ complying with the secondary lobe-free radiation condition, a full 180º beam steering requires a minimum dispersion $|D|_{min}L = 58\ ps/nm$, according to the maximum beam condition (7). Considering standard DCF with distributed dispersion coefficient $D = -85\ ps/(nm \cdot Km)$, it corresponds to roughly $0.68\ Km$. In order to focus the study towards an experimental test, the values have been adapted to the available resources, yielding an inter-element spacing $d = 4\lambda/5$ at $8\ GHz$ and a dispersion of $DL = -340\ ps/nm$. Figure 6 shows the Array Factors resulting from tuning the relative progressive wavelength shift $\delta\lambda_0$ and table II lists the required delays.

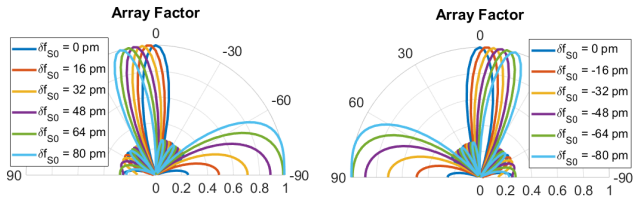

(a) (b)

Fig. 6. Array Factor diagram for a relative progressive wavelength shift $\delta\lambda_0 > 0$ (a) and $\delta\lambda_0 < 0$ (b).

The lobe-free operation is limited to ± 14º, which implies a theoretical relative progressive wavelength shift of $\delta\lambda_0 = \pm 73.5\ pm$. It can be observed that performing a simulation with a relative progressive wavelength shift $\delta\lambda_0 = 80\ pm$, a second lobe with the same amplitude of the primary one shows up, proving the restriction.

TABLE II
Summary of delays and wavelengths for an array of $N = 4$ PAAE.

i	Compensating Delay (T_i)	Geometrical Delay ($\Delta\tau_{Gi}$)	Wavelength shift ($\delta\lambda_i$)
1	$0\ ns$	$-0.15\sin(\theta)\ ns$	$0.45\sin(\theta)\ nm$
2	$0.54\ ns$	$-0.05\sin(\theta)\ ns$	$0.15\sin(\theta)\ nm$
3	$1.08\ ns$	$0.05\sin(\theta)\ ns$	$-0.15\sin(\theta)\ nm$
4	$1.62\ ns$	$0.15\sin(\theta)\ ns$	$-0.45\sin(\theta)\ nm$

In order to obtain a flat response around the frequency band, the bias is optimized using the condition (10). It is observed how the Quadrature Point (QP) biasing $\theta_B = \pi/2$ in Figure 7(a) results in significant CD fading amplitude penalty of around 5.1 dB, when the RF frequency is shifted from 7 GHz to 9 GHz. In order to shift the CD-fading free band the MZM is biased at $\theta_B = 1.35\pi$, resulting in the flattened amplitude response shown on Figure 7(b).

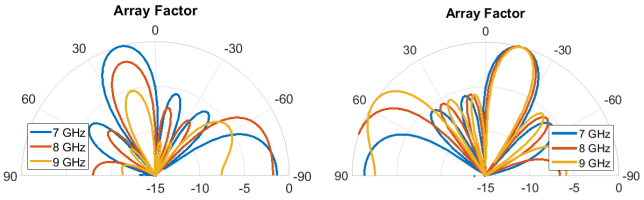

(a) (b)

Fig. 7. Array Factor diagrams for $\theta_B = \pi/2$ (a) and $\theta_B = 1.35\pi$ (b).

V. Conclusions

We have presented a proposal for an optical network to control the direction of maximum directivity of a PAA. The beam steering is achieved through wavelength tuning of an array of input lasers, and dispersive propagation. The simulation results show the ability of the biasing technique to avoid the CD-fading penalty and enable large bandwidth and high count PAAs. The method is tunable, allowing to reconfigure the target frequency band. The free-lobe beam steering operation is mainly restricted by the PAA inter-elements spacing, which will also determine the maximum pointing direction along with the AWG channel bandwidth.

Acknowledgements

This work was partly funded by the Ministerio de Ciencia e Innovacion (MICINN) under projects TEC2016-78028-C3-1-P, PID 2019-107885GB-C31, MDM2016-0600, and Catalan Research Group 2017 SGR 219.

References

[1] X. Ye, D. Zhu, Y. Zhang, S. Li, and S. Pan, "Analysis of Photonics-Based RF Beamforming With Large Instantaneous Bandwidth," in *J. Of Lightwave Technol.*, vol. 35, pp. 5010 - 5019, Dec. 2017.

[2] L. Jofre, C. Stoltidou, S. Blanch, T. Mengual, B. Vidal, J. Marti, I. McKenzie, and J.M. del Cura, "Optically beamformed wideband array performance," in *IEEE Trans. on Antennas and Propagation*, Vol. 56, n. 6, pp.1594-1604, Jun. 2008.

[3] B. G. Kim, S. H. Bae, H. Kim, and Yun C. Chung,"RoF-Based Mobile Fronthaul Networks Implemented by Using DML and EML for 5G Wireless Communication Systems," in *J. Of Lightwave Technol.*, vol. 36, pp. 2874 - 2881, July 2018.

[4] J. L. Corral, J. Marti and J. M. Fuster, "Optical Up-Conversion on Continuously Variable True-Time-Delay Lines Based on Chirped Fiber Gratings for Millimeter-Wave Optical Beamforming Networks," in *IEEE Trans. Microwave Theory Tech*, vol. 47, pp. 1315 - 1320, July 1999.

[5] J. Tabares, S. Ghasemi, V. Polo, and J. Prat, "Simplified Carrier Recovery for Intradyne Optical PSK Receivers in udWDM-PON," in *J. Of Lightwave Technol.*, vol. 36, pp. 2941 - 2947, July 2018.

[6] Y. Gao, A. Wen, Y. Chen, S. Xiang, H. Zhang, and L. Shang, "An Analog Photonic Link With Compensation of Dispersion-Induced Power Fading," in *IEEE Photon. Technol. Letters*, Vol. 27, No. 12, June 15, 2015.

[7] C. A. Balanis, "Antenna Theory: Analysis and Design," , pp. 283 - 385, Wiley, 2005.

[8] P. S. Devgan, D. P. Brown, and R. L. Nelson "RF Performance of Single Sideband Modulation Versus Dual Sideband Modulation in a Photonic Link," in *J. Of Lightwave Technol.*, vol. 33, May 2015.

[9] J. L. Corral, J. Marti, J. M. Fuster, and R. I. Laming, "Dispersion induced bandwidth limitation of variable true time delay lines based on linearly chirped fiber gratings," in *Electron. Lett.*, vol. 34, no. 2, pp. 209–211, 1998.